Arch. Mech., 38, 5–6, pp. 635–645, Warszawa 1986

Large-scale vortices inside a confined mixing layer Formation conditions and evolution(*)

D. KHELIF, M. GERON and J. L. BOUSGARBIES (POITIERS)

FLOW VISUALIZATION motion pictures of side, top and span views in a plane confined mixing layer were performed. The formation of vortical coherent structures and their further evolution were observed and filmed for several values of the characteristic parameters $\lambda = U_2/U_1$ and $\Delta U = U_1 - U_2$. The influence of these two parameters on the appearance of the vortices and their subsequent evolution was investigated. A statistical analysis of digitized flow pictures has permitted to determine the mean position of the birth of the vortices and to follow thoroughly their evolution.

Wykonano zdjęcia filmowe w kilku ujęciach dla płaskiej ograniczonej warstwy mieszania. Zaobserwowano i sfilmowano proces tworzenia się koherentnych struktur wirowych oraz ich ewolucję przy różnych wartościach parametrów charakterystycznych $\lambda = U_2/U_1$ i $\Delta U = U_1 - U_2$. Zbadano wpływ tych dwóch parametrów na powstawanie i dalszą ewolucję wirów. Analiza statystyczna cyfrowych obrazów przepływu pozwoliła na ustalenie miejsca narodzin wirów i na dokładne prześledzenie ich dalszej ewolucji.

Произведены киносъемки в нескольких подходах для плоского ограниченного слоя смешивания. Наблюдался и снимался процесс образования когерентных вихревых структур, а также их эволюция при разных значениях характеристических параметров $\lambda = U_2/U_1$ и $\Delta U = U_1 - U_2$. Исследовано влияние этих двух параметров на возникновение и дальнейшую эволюцию вихрей. Статистический анализ цифровых изображений течения позволил установить место рождения вихрей и точно следить их дальнейшую эволюцию.

1. Introduction

SINCE the discovery of coherent structures in the turbulent mixing layer by BROWN and ROSHKO [4, 5] both theoretical and experimental investigations devoted to this area have considerably increased.

Among those investigations we can cite ROSHKO [13] who studied statistically the random properties of coherent structures in turbulent shear flows. The pairing phenomena which is an amalgamation of two adjacent eddies was studied at low and moderate Reynolds numbers by WINANT and BROWAND [14]. A more complex form of amalgamation where more than two vortices interact was observed by ROSHKO [13], DIMOTAKIS and BROWN [8] and also in a forced mixing layer by HO and HUANG [10]. Dimotakis and Brown reported the tearing process, a vortical structure is absorbed by its neighbouring vortices. The tearing was observed by us at high Reynolds numbers.

KONRAD [12] and BREIDENTHAL [3] studied the mixing transition which is characterized by the appearance of smaller scale three-dimensional structures. BERNAL [1] explored sta-

(*) Paper gives at XVII Symposium on Advanced Problems and Methods in Fluid Mechanics, Sobieszewo, 2–6 September 1985.

tistically the primary vortex structures and the secondary three-dimensional structures. HERNAN and JIMENEZ [9] extracted quantitative information from the flow pictures by a digital image analysis. A three-dimensional model of the plane mixing layer was constructed by JIMENEZ, COGOLLOS and BERNAL [11] by applying a digital image processing.

Our study differs somewhat from most of the earlier works for it concerns a shear mixing layer when it is confined by walls whereas the studies related before concern free shear layers. That allows us to understand more specifically the behaviour of the mixing flow in combustion chambers as well as many other technological applications of the mixing where it is usually confined by walls.

The first part of this work is an attempt to determine the flow parameters which should control the appearance and the evolution of the vortices observed in the mixing layer. One can predict that the fundamental parameters, the initial stream velocity ratio $\lambda = U_2/U_1$ and the difference between these two velocities $\Delta U = U_1 - U_2$ would be influential factors. The influence of these parameters has been experimentally studied by means of flow visualization motion pictures.

The second step concerns the thorough study of the life history of the coherent structures, from their birth until their disappearance. Sixteen mm movies were used to gain more detailed information concerning the individual evolution of the vortices. The lifetime histories of the vortices were determined and a statistical study was performed.

2. Experimental device

The turbulent mixing layer is established between two streams of water separated by a splitter plate. This thin splitter plate is a wedge of 3.5° total angle whose trailing edge thickness is less than 0.1 mm.

The test section is 2 cm high, 10 cm wide and 30 cm long. The upstream part of the hydraulic device is a modified version of that used in a previous work, COLLIN [6]. The two streams cross a bed of small marbles in the settling chamber and then cross screens in each side of the splitter plate before they begin to mix together at its trailing edge. So they are of equal thickness ($e = 1$ cm), parallel, uniform and with different velocities U_1 and U_2. These two velocities are controlled by accurate flowmeters and could be varied from 1 cm/s to 22 cm/s. A more detailed description is given elsewhere, COLLIN [6].

3. Flow visualization technique

The flow visualization technique is similar to the classical one described by DIMOTAKIS [7] with a slight difference. This difference is that the laser beam is passed through a combination of two spherical lenses instead of one and a cylindrical lens. The light sheet produced by this optical set is about 1 mm in thickness and 30 cm in the streamwise direction.

The two spherical converging lenses with their different focusing lengths act like a zoom and allow to focus the light sheet at any distance from the laser source. This light sheet can be oriented in three orthogonal directions which correspond respectively to the side, upper and cross sections of the flow.

In order to observe the flow pattern in the mixing layer, phenolphtaleine is added to the low speed stream (about 100 g/m^3) so that the relative variation in density is less than 0.04%.

For the purpose of investigating the birth and the evolution of the vortices, the configuration thus observed was both photographed and recorded by a videoscope and on 16 mm sequences. The frame rate of the 16 mm camera was 24 pictures per second what corresponds to exposure time equal to 1/188 s. The video camera takes 50 pictures every second.

4. Results

4.1. Flow configuration and influence of the main parameters on the life of the vortices

The influence of the main parameters of the flow λ and ΔU on the lifetime of the vortices was studied by means of flow visualizations which were performed for several values of these parameters. An example of the flow configuration obtained is presented in Figs. 1 and 2.

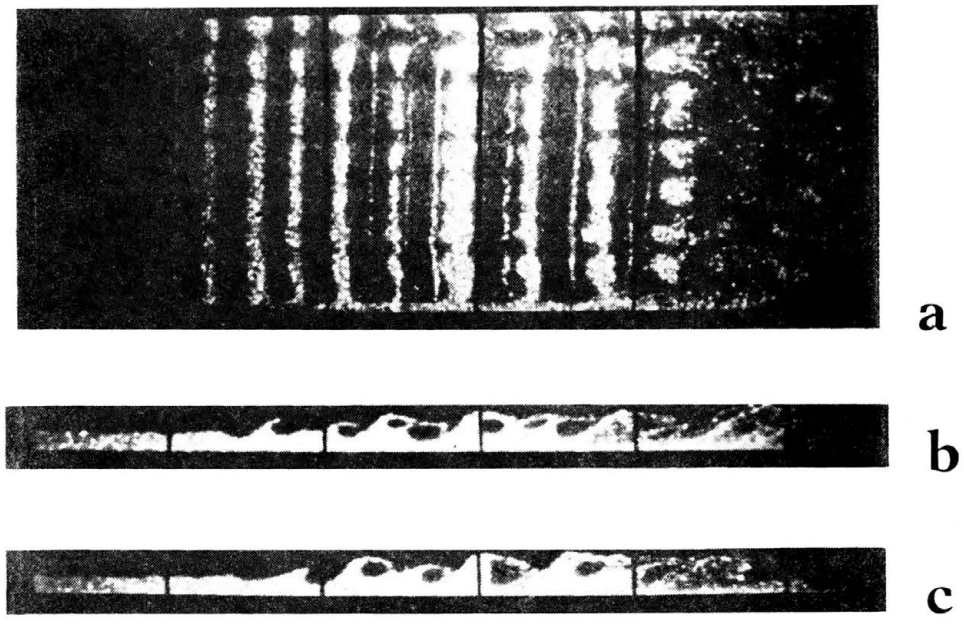

FIG. 1. Top (a) and side (b) and (c) views of the flow $U_1 = 13$ cm/s, $U_2 = 6.5$ cm/s, $\mathrm{Re}_x/x = 643/\mathrm{cm}$ — $\mathrm{Re}_m = 1930$.

Figures 1b and 1c are the side views of the flow configuration observed in the mixing layer. The flow is from the left to the right. The lower layer which is the lower velocity stream, is coloured by phenolptaleine (white). The trailling edge of the splitter plate is at the extreme left of each picture and the distance between the vertical black streaks is 5 cm.

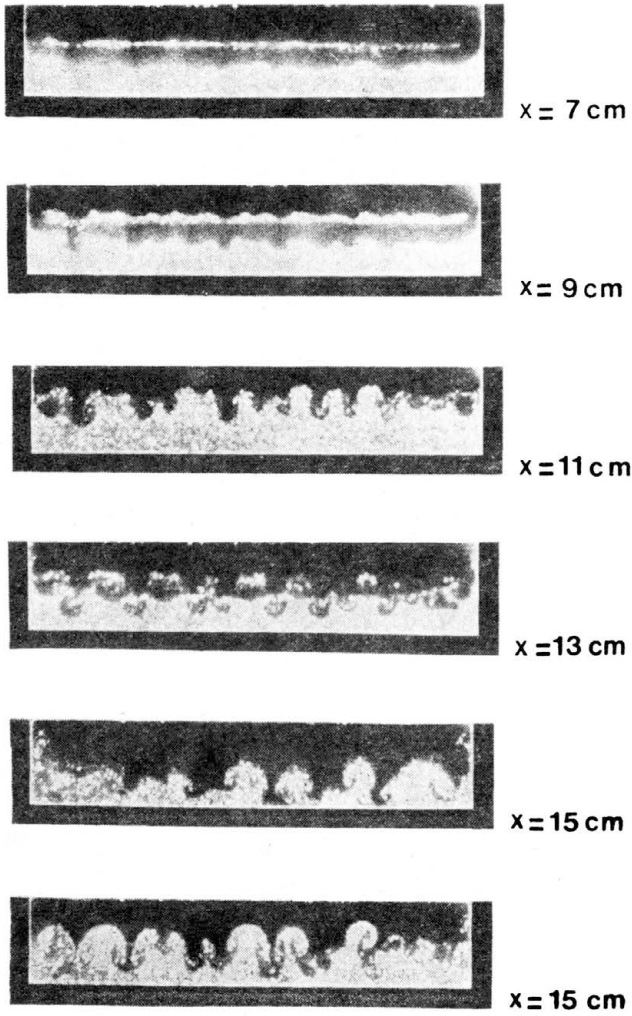

FIG. 2. Cross views of the mixing layer at several downstream locations (for same parameters as in Fig. 1).

The elapsed time between these two pictures is 7/12 s. The two adjacent vortices which are pairing at $x = 12.5$ cm in Fig. 1b give a larger resulting vortex at $x = 16$ cm (Fig. 1c). In the upstream part of the mixing layer ($x < 12$ cm) the coherent structures are two-dimensional, as it is clearly illustrated by the top view presented in Fig. 1a. Downstream of this region, spanwise disturbance appears and increases as the vortices are convected through out the length of the layer. This lateral undulation gives streamwise streaks observed by KONRAD [12] and BREIDENTHAL [3].

The cross sections of the flow presented in Fig. 2 allow to follow the evolution of the streaks and the streamwise vortices with which they are associated (BERNAL [1]). The separate influence of each parameter was provided by the analysis of videoscope side view sequences. Sequences where ΔU was fixed while λ varied and other sequences where λ was fixed while ΔU varied. Figure 3 shows the results obtained for $\Delta U = 7$ cm/s and λ

varying from 0.18 to 0.62. The x-location of creation of vortices and the pairing of two neighbouring vortices are plotted as a function of λ. It is interesting to note that both of these two features do not occur at a fixed abscissa, but between two extreme locations. Thus it was possible to determine x-segments where the birth and the pairing were observed.

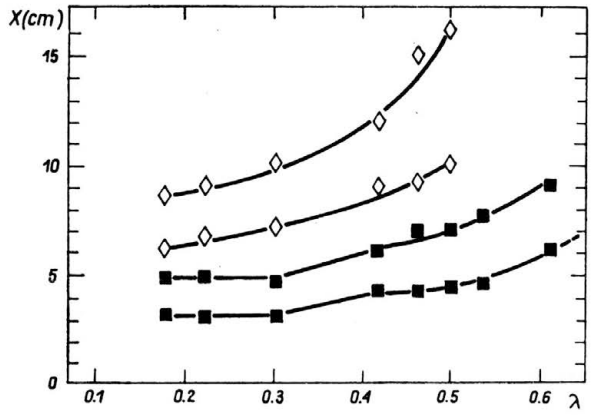

FIG. 3. x locations of the appearance of the vortices ■, and of the pairing ◇, as a function of λ when $\Delta U = 7$ cm/s.

Their mean locations are an increasing function of λ. This means that a reduction of the shearing (an increase of λ) makes those features occur far downstream of the origin of the mixing layer. In a extreme case when $U_1 = U_2$ (ie $\lambda = 1$) the interface between the two

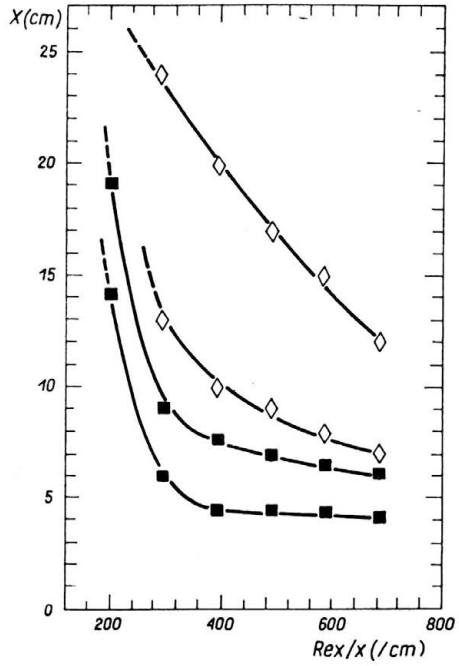

FIG. 4. x locations of the appearance of the vortices ■ and of the pairing ◇ as a function of $\mathrm{Re}_x/x = \Delta U/\nu$ when $\lambda = 0.5$.

streams is not perturbed, it remains even throughout the length of the test section and the structures do not appear.

For $\lambda = 0.5$, the variations of the downstream position of both the birth of the eddies and their amalgamations are plotted as a function of $\mathrm{Re}_x/x = \Delta U/\nu$, in Fig. 4. In the test section of our experimental device the coherent structures do not appear for Re_x/x less than 200. When Re_x/x reached this value it was possible to observe the appearance of the eddies far downstream (between 14 cm and 19 cm); however, the pairing has not been observed yet. In the region where $200 < \mathrm{Re}_x/x < 400$ a little increase of ΔU causes a strong decrease of the downstream locations of birth and pairing. For Re_x/x greater than 400 the x-location of the birth decreases slowly while the amalgamation x-location undergoes a more marked decrease.

As one can see, analysis of the videoscope sequences allows a rough understanding of the distinct influence of λ and ΔU on the further behaviour of the vortices. Each of those two parameters influences the life history of the eddies but neither λ nor ΔU control them totally. The accuracy of the x-measurements was about 0.5 cm because of random properties of the eddies and the different errors introduced by the video set (camera, TV screen, the human operator, etc.).

4.2. Study of the individual evolution of the vortices

A statistical process of the filmed sequences corresponding to the same velocity ratio λ and to two different values of ΔU was performed. Some more detailed knowledge on the

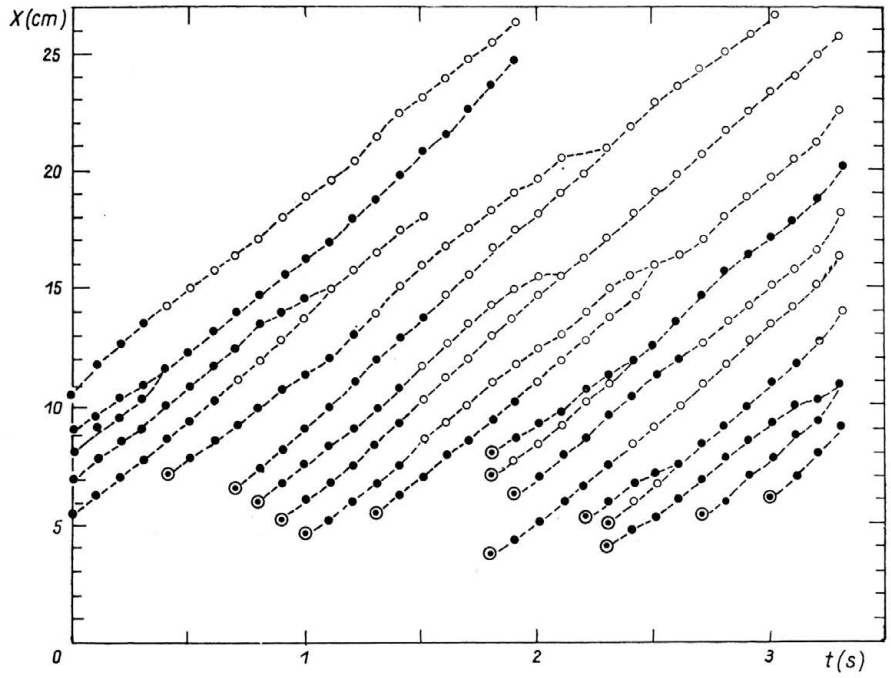

FIG. 5. (x, t) diagram of the life of vortices ($U_1 = 8$ cm/s; $U_2 = 4$ cm/s; $\mathrm{Re}_x/x = 400$/cm; $\mathrm{Re}_m = 1190$); ⊙ birth of a vortex, ● open vortex, ◯ rolled up vortex.

behaviour of the coherent structures during their lifetime is provided by this study. Those sequences were digitized (BONNET [2]) and each vortex was tracked frame by frame. An $x-t$ diagram of the time history of the vortices involved was obtained. An example corresponding to the processing of 80 consecutive frames (3.3 s) for $U_1 = 8$ cm/s and $U_2 = 4$ cm/s, is given in Fig. 5. The eddies could be divided into two classes: open vortices or OV (see Fig. 1b at $x = 8$ cm and $x = 11$ cm) and rolled up vortices or RV (see Fig. 1b at $x = 15.5$ cm). The OV is the primary shape of RV; nevertheless, some structures remain OV until their disappearance far downstream, as can be seen in the above diagram. From these remarks one can distiguish four kinds of pairing. Each one differs from the others according to the class of the vortices which pair together. The pairing could happen between:

OV-OV,

OV-RV,

RV-RV,

RV-OV.

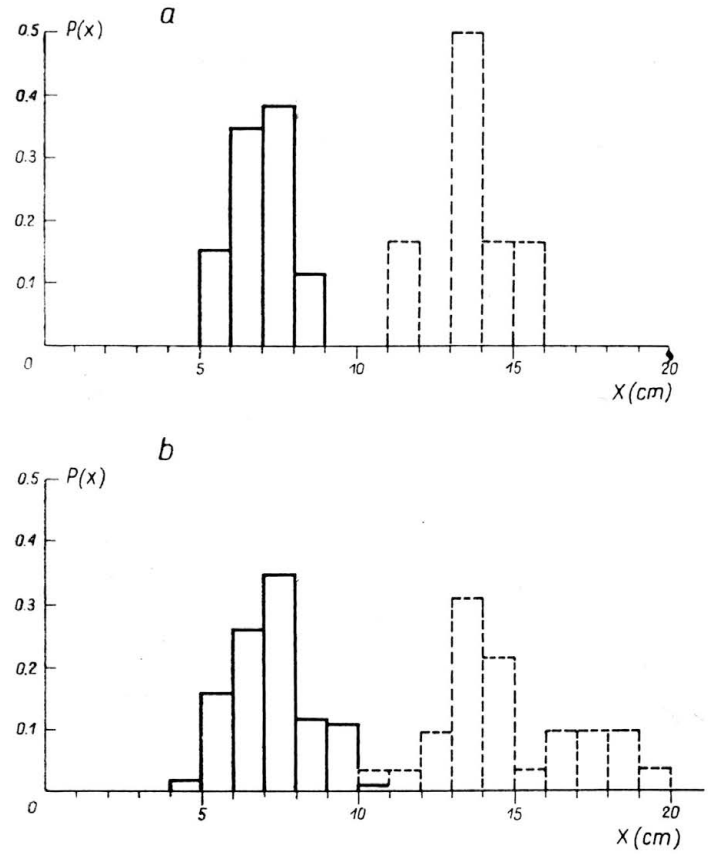

FIG. 6. Probability distribution of the x location of the appearance of vortices (—) and of the pairing (- - -); a) 80 frames sample, b) 500 frames sample.

The resulting vortex was always OV for OV-OV pairing and RV for RV-RV pairing. The OV-RV pairing could give OV or RV as resulting vortex. However, it was observed that RV-OV pairing gives only RV.

For $U_1 = 13$ cm/s and $U_2 = 6.5$ cm/s, two sequences were digitized and processed. The short one is 80 frames and the longer is a sequence of 500 frames from which 134 life histories of the vortices had been determined. The probability distribution of the x-location of both the birth and pairing phenomena is presented for each sample in Figs 6a and 6b. Comparison of the results obtained from the two samples reveals that the determination of the locations of birth and pairing is roughly but correctly provided by the short sequence. Long sequences are used only if one needs to have an improved $P(x)$ distribution; this remark is especially true for the pairing.

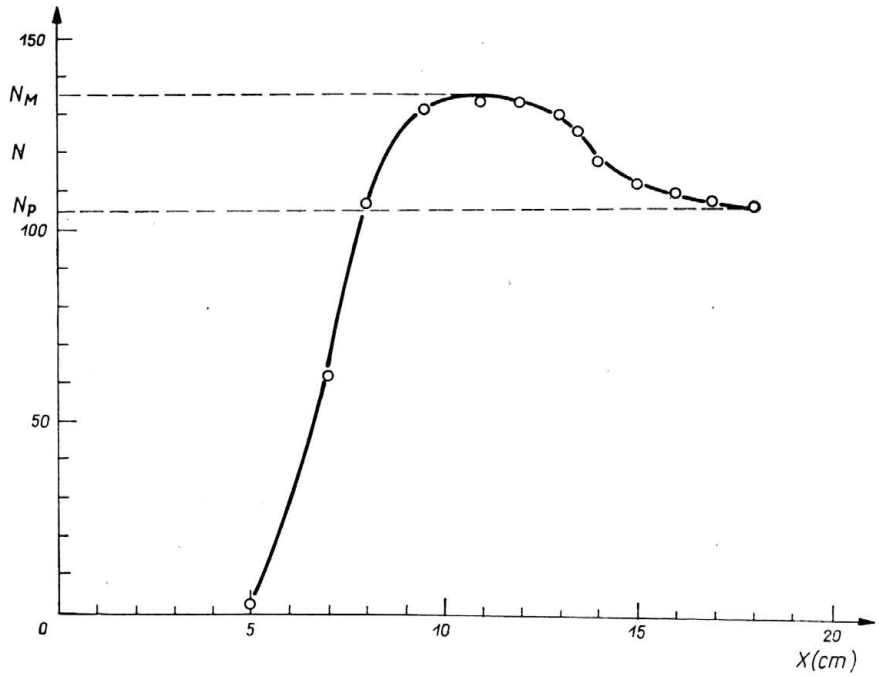

FIG. 7. Number of vortices as function of x from the long film sequence $U_1 = 13$ cm/s; $U_2 = 6.5$cm/s.

In Fig. 7 the evolution of the total number N of vortices observed during the examination of the longer sequence is plotted as a function of the downstream position x. The coherent structures do not appear before $x = 5$ cm. The strong increase of N between $x = 5$ and $x = 9.5$ cm can be approximated by a linear growth. Thus the measured linear growth rate is $dN/dx = 30$ vortices/cm. This corresponds to the birth region. N is quite constant between $x = 9.5$ cm and $x = 12$ cm. In this intermediate region the increase of N caused by the birth of new vortices is balanced by the loss of vortices during the pairing phenomenon. This is well confirmed by Fig. 6b. For $x > 13$ cm N grows gradually less as a result of pairing processes. In this region the probability of pairing is at its maximum and no new eddy appears.

The pairing rate, p, defined as the ratio between the number of vortex amalgamations and the total number of vortices N, was inferred from the previous curve by the relation

$$p = (N_M - N_p)/N_M = 0.22.$$

This loss of vortices is accompanied by a diminution of the passing frequency of the eddies. For the present experimental conditions this frequency decreases from 7H to 5H, as it is shown by the frequency spectra deduced from the measurements and presented in Fig. 8a. This frequency decreases from 5H to 4H when the initial stream velocities were $U_1 = 8$ cm/s and $U_2 = 4$ cm/s, Fig. 8b.

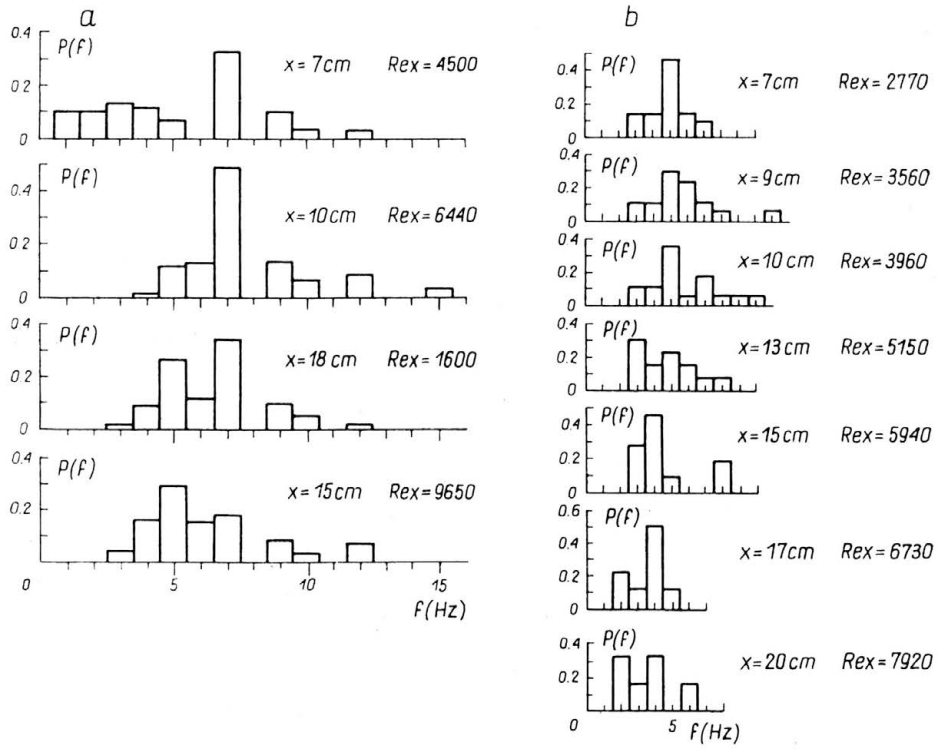

FIG. 8. Passing frequency of the vortices: probability distribution at different downstream locations; a) $U_1 = 13$ cm/s; $U_2 = 6.5$ cm/s, b) $U_1 = 8$ cm/s; $U_2 = 4$ cm/s.

4.2. Convection velocity of the vortices

The mean velocity at which the coherent structures were convected downstream deduced from the $x-t$ diagram was found $U_c = 8.30$ cm/s. This mean value is about 40% higher than the mean velocity of the flow which is $U_m = 6$ cm/s. BERNAL [1] has found U_c 5% higher than U_m. This large discrepancy can be explained by the fact that the mixing layer studied here is confined by walls. The examination of the mean velocity profile at the origin of the mixing layer reveals the presence of well-grown boundary layers on the side walls and on each side of the splitter plate. The loss of velocity in the boundary layers is balanced by an important increase of the mean velocity in the central region of each

stream: $U_{1a} = 9.7$ cm/s and $U_{2a} = 5.2$ cm/s for U_1 and U_2, respectively. These velocities are the actual initial stream velocities which should be considered in the calculation of the different parameters of the mixing layer. Thus the actual mean velocity of the flow in the mixing zone is 7.45 cm/s and finally

$$(U_c - U_{ma})/U_m = 0.07$$

is in good agreement with Bernal's value. The growth of the boundary layers was favoured by the fact that the velocities streams were very weak. When these velocities were $U_1 = 13$ cm/s and $U_2 = 6.5$ cm/s the boundary layers were less developed than in the previous case. The mean velocity at which the eddies were convected was found 10% higher than U_m.

5. Conclusion

The examination of sequences obtained during flow visualization performed in a mixing layer shows that the formation of vortex structures and the subsequent phenomenon are only quasiperiodic. The statistical study of movie sequences corresponding to several values of the initial flow velocity ratio allows to obtain the probability distribution of the location of both the appearance of two-dimensional vortex structures and the pairing between two adjacent vortices. The mean locations of these two main phenomena are increasing functions of the velocity ratio and decreasing functions of the velocity difference.

The mean velocity at which the vortices are convected throughout the confined mixing layer is found higher than the mean velocity of the flow. This is an illustration of the important role played by the constraining walls.

For $\lambda = 0.5$ and $\Delta U = 6.5$ cm/s, the pairing rate, p, defined as the ratio between the number of vortex amalgamations and the total number of vortices is found to be about 0.2. This value is lower than that found by BERNAL [1] ($p = 0.66$) corresponding to a higher shear inside the mixing zone. For the purpose of determining the dependence of the pairing rate on the flow parameters, further experiments are projected.

This work was supported by the CNRS (A.T.P. Dynamique des Fluides Géophysiques et Astrophysiques).

References

1. L. P. BERNAL, *The coherent structures of turbulent mixing layers. 1. Similarity of the primary vortex structure. 2. Secondary streamwise vortex structure*, Ph. D. Thesis, California Institute of Technology, 1981.
2. J. P. BONNET, J. L. BOUSGARBIES, E. CHAPUT, D. KHELIF, *Application d'une méthode de traitement numérique d'images à l'étude de la structure d'une zone de mélange*, Colloque National de Visualisation et de Traitement d'Images, Nancy, Janvier 1985.
3. R. E. BREIDENTHAL, *A chemically reacting turbulent shear layer*, Ph. D. Thesis, California Institute of Technology, 1978.
4. G. L. BROWN and A. ROSHKO, *The effect of density difference on the turbulent mixing layer*, Agard CP 93, 23-1 to 23-11, 1971.

5. G. L. BROWN and A. ROSHKO, *On density effects and large structure in turbulent mixing layers*, J. Fluid Mech., **64**, 775–816, 1974.
6. A. COLLIN, *Contribution à l'étude expérimentale de l'hydrodynamique et du transfert de matière au sein d'une zone de mélange plane confinée*, These de Doctorat de 3ème cycle, Université de Poitiers 1984.
7. P. E. DIMOTAKIS, F. D. DEBUSSY and A. KOOCHESFAHANI, *Particle streak velocity field measurements in a two-dimensional mixing layer*, Ph. Fluids, **24**, 6, June 1981.
8. P.E. DIMOTAKIS and G. L. BROWN, *The mixing layer at high Reynolds number. Large structure dynamics and entrainment*, J. Fluid Mech., **78**, 535–560, 1976.
9. M. A. HERNAN and J. JIMENEZ, *Computer analysis of a high speed film of the plane turbulent mixing layer*, J. Fluid Mech., 119, 323–345, 1982.
10. C. M. HO and L. S. HUANG, *Subharmonics and vortex merging in mixing layers*, J. Fluid Mech., 119, 443–473, 1982.
11. J. JIMENEZ, M. COGOLLOS and L. P. BERNAL, *A perspective view of the plane mixing layer*, J. Fluid Mech., 152, 125–143 1985.
12. J. H. KONRAD, *An experimental investigation of mixing in two-dimensional turbulent shear flows with application to diffusion limited chemical reactions*, Ph. D. Thesis California Institute of Technology, 1976.
13. A. ROSHKO, *Structure of turbulent shear flows*, A.I.A.A. Journal, **14**, 1349–1357, 1976.
14. C. D. WINANT and F. K. BROWAND, *Vortex pairing: the mechanism of turbulent mixing layer growth at moderate Reynolds number*, J. Fluid Mech., 63, 237–255, 1974.

LABORATOIRE D'ETUDES AÉRODYNAMIQUES, POITIERS, FRANCE.

Received January 8, 1986.